DEPARTMENT OF DEFENCE
DEFENCE SCIENCE & TECHNOLOGY ORGANISATION
DSTO

Measurement of the Natural Bending Modes of Rotors in the TF30 Engine

Mark Shilo
and
Andrew Becker

DSTO-TN-0393

Measurement of the Natural Bending Modes of Rotors in the TF30 Engine

Mark Shilo and Andrew Becker

Airframes and Engines Division
Aeronautical and Maritime Research Laboratory

DSTO-TN-0393

ABSTRACT

The natural bending modes of the high and low speed shafts from the TF30 engine were measured in order to provide an unequivocal reference for validation of 3D Finite Element models of the shafts. The shafts were assembled separately, and without blades or any engine casing structure.

Published by

DSTO Aeronautical and Maritime Research Laboratory
506 Lorimer St
Fishermans Bend, 3207, Vic. Australia

Telephone: (03) 9626 7000
Fax: (03) 9626 7999

AR-012-009
September 2001

APPROVED FOR PUBLIC RELEASE

Measurement of the Natural Bending Modes of Rotors in the TF30 Engine

Executive Summary

Measurements were made of TF30 P103 engine rotors to determine the natural bending mode shapes and the frequencies at which they occurred. The purpose of the measurements was to assist with validation of Finite Element models of the TF30 shafts. The models were developed for component fatigue and lifing analyses, but cannot be used with confidence until they are validated against measurements of the actual shafts.

The rotor components were sourced from surplus and unserviceable stock at RAAF Amberley, and were assembled at AMRL. To facilitate measurement, the shafts were assembled separately, exclusive of any engine casing structure and blades. (Normally, the rotors are assembled concentrically, and integrally with the engine casing structure.)

To achieve a support that enabled unconstrained bending motion of the shafts they were supported by suspending them vertically from the ceiling by a light cable. In this manner only the axial movement is restrained (against gravity), leaving free the natural longitudinal movement. The natural bending modes were excited with a sharp impulse introduced with a wooden mallet, and measured using accelerometers.

The measurements clearly identified the bending modes of both the shafts, and the frequencies at which they occurred. The Finite Element models of the shafts can now be compared to the real measurements and adjusted as necessary.

These validated models will assist in the sole operator support of the F-111.

Contents

1. Introduction

To increase the understanding of engine component fatigue and failure in support of airworthiness management, a 3D FE model of a whole rotor system has been developed for the TF30 engine. The model consists of 49 essential mechanical components with various temperature-dependent material properties, and will be used for fatigue failure investigation and life management of the TF30 engine components.

However, before the results of these analyses can be used with confidence, the dynamic response behaviour of the model needs to be validated against the dynamic response of actual TF30 rotors. To achieve this validation, high and low speed TF30 engine rotors were sourced from RAAF Amberley, assembled at DSTO, and dynamically tested.

Measurements of the natural frequencies of the bending modes of the high and low speed TF30 engine rotors have been taken at AMRL. These measurements form a reference against which the performance of the model can be compared. This report describes the measurement procedure and presents the results for reference.

2. Construction of rotors

2.1 Collection of components

The components needed for complete assembly of the rotors were identified on engineering drawings and Illustrated Parts Breakdown (IPB)[1] manuals. The components used were at the end of their service life, and surplus to RAAF requirements. Collected over a period of months at RAAF Amberley as they were discarded through the breakdown to spares program, the components were freighted to DSTO in October 2000.

2.2 Assembly

Assembly was achieved with the aid of the engineering drawings, IPB, and the part numbers and identification tags on the components themselves.

At 501 Wing RAAF Amberley, routine engine rebuilds after deeper level maintenance involve the rotors being assembled integrally with the compressor and turbine cases. However, as the dynamic modal response measurements at AMRL required the shafts to be assembled separately and without engine casing structure, RAAF standard operating procedures could not be used. Unconventional approaches therefore had to be developed to achieve correctly assembled rotors.

---

[1] Defence Instruction (Air Force) AAP 7112.002-4, Illustrated Parts Breakdown, TF30 Engine. Date of issue 2 Jan 1991.

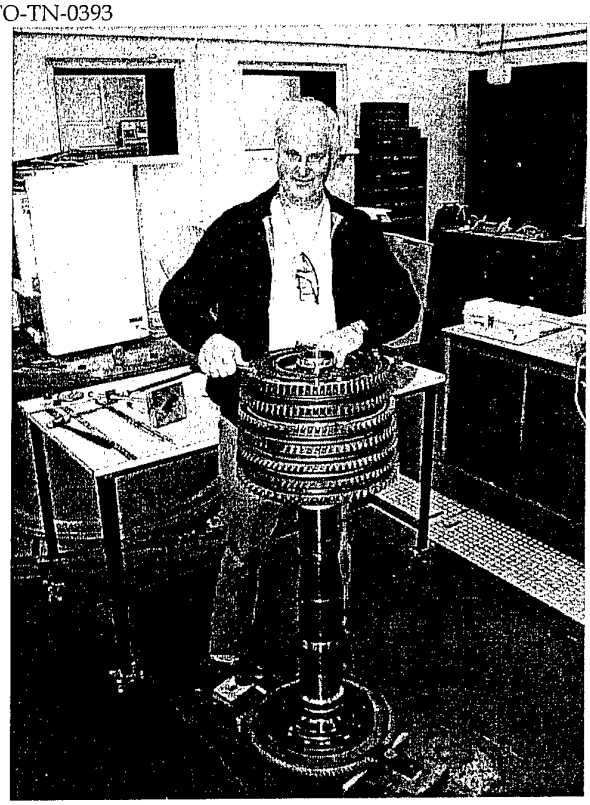

Figure 1. Assembling high speed rotor.

2.3 Exclusions

To facilitate assembly and handling, the rotors were assembled without compressor or turbine blades. While this does have a measurable effect on the bending modes of the shafts, the blades can readily be added or removed from the finite element models of the rotors.

In addition, there were four components that were not included in the final assembly of the low speed rotor. These were:

- Oil/Air transfer tube (N1),
- Turbine shaft lock (N2),
- Tie rod shield, rear compressor (N2), and
- Turbine air seal (N2)

These components were excluded because of the difficulty involved with correct fitment and lack of some specialised tooling. The exclusion of these four components is expected to make negligible difference to the results because they are very small and light compared to the rest of the rotor, and they do not provide structural stiffness. Figure 2 shows the excluded components.

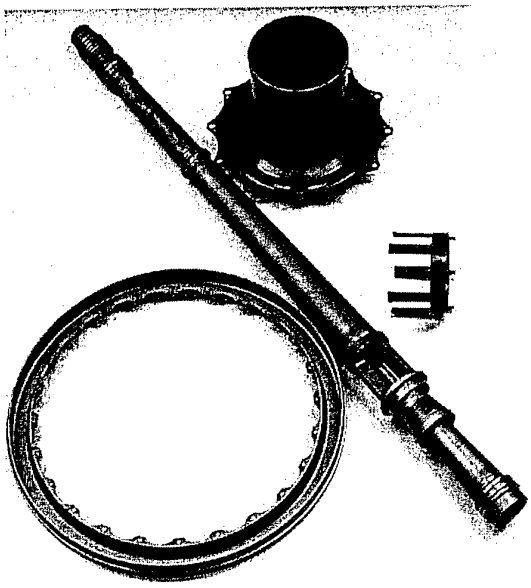

Figure 2. Components excluded from shaft assemblies.

3. Setup

3.1 Dimensioning the rotors

In order to accurately determine and animate the mode shapes of the N1 (low speed) and N2 (high speed) rotors, the intended measurement points were marked off on each rotor (measured from the shaft extremity). This then enabled the vibration magnitude and phase measurements (relative to a reference accelerometer) to be attributed to specific locations on the rotors, permitting representation as a modal picture of the rotor. This seemingly simple task proved to be more difficult than first expected, primarily due to the non-uniform shape of the rotor sections.

In order to mark off the measurement locations, the tape measure was placed parallel to the rotor and a T-square used to affiliate the measurement locations with a corresponding reading on the tape measure. Figure 3 shows the location measurement setup. Convenient measurement locations for the turbine and compressor sections were selected according to the availability of flat, machined surfaces that could accept the physical dimensions of the accelerometer. Figure 4 shows a close-up of some accelerometer measurement locations. The shaft section between the turbine section and the compressor section was sufficiently uniform to allow measurement locations to be spaced at 100mm intervals.

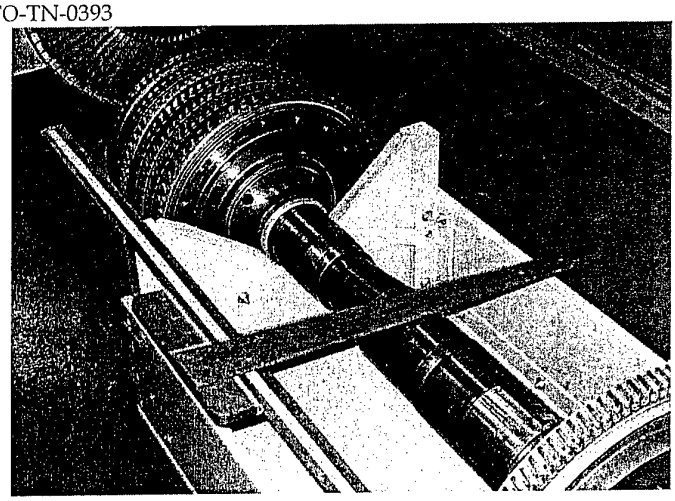

Figure 3. Location measurement setup.

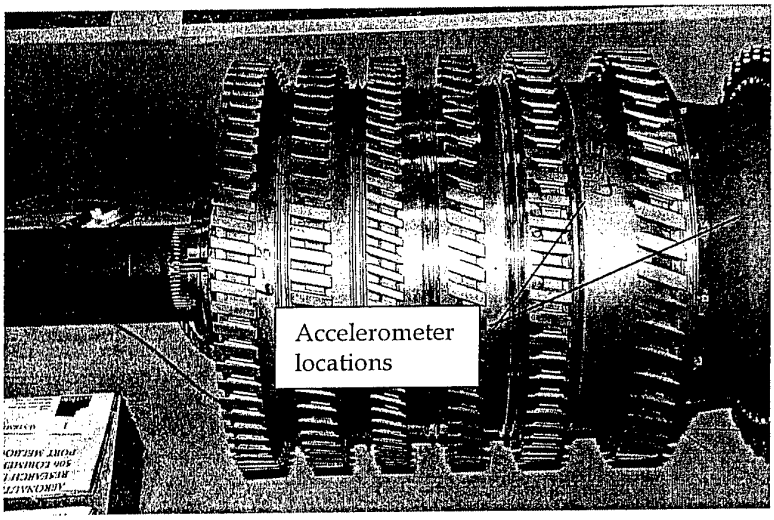

Figure 4. Close up of accelerometer measurement locations on N1 compressor.

The geometry of the N1 rotor made it convenient to measure all of the accelerometer locations from the turbine end of the shaft, whereas the accelerometer locations on the N2 shaft were measured from the compressor end.

3.2 Supporting the rotors

In order to achieve "free-free" natural bending motion, the shafts were supported in a way that permitted unconstrained longitudinal bending vibration. This was achieved by suspending the rotor vertically on a thin steel cable. Figure 5 shows the plate and eyebolt assembly that was used to connect the cable to the lower end of the rotor shaft. The 3mm diameter cable was then passed through the hollow core of the rotor shaft and connected to a gantry-hoist hook. A cable spacer was employed at the upper end to steady the suspended rotor. Figure 6 shows the two-part spacer that was made to

centre the cable at the upper end. The same method of suspension was employed for both the N1 and N2 rotors.

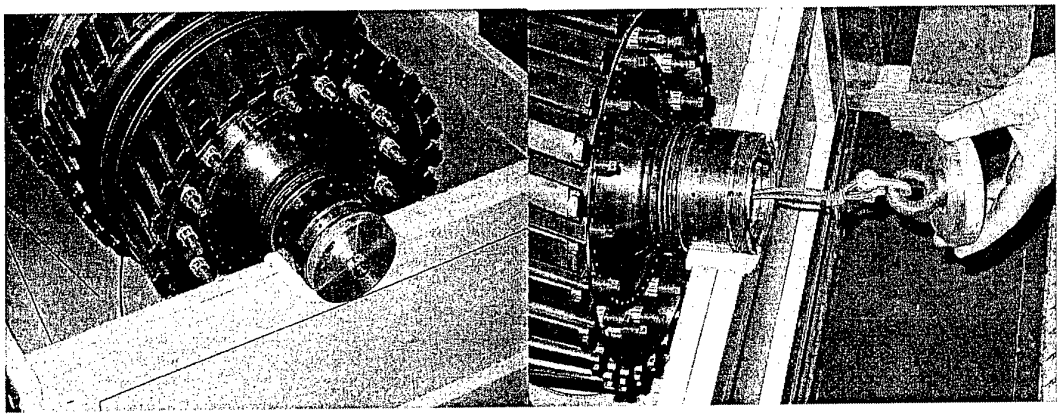

Figure 5. Shaft support assembly

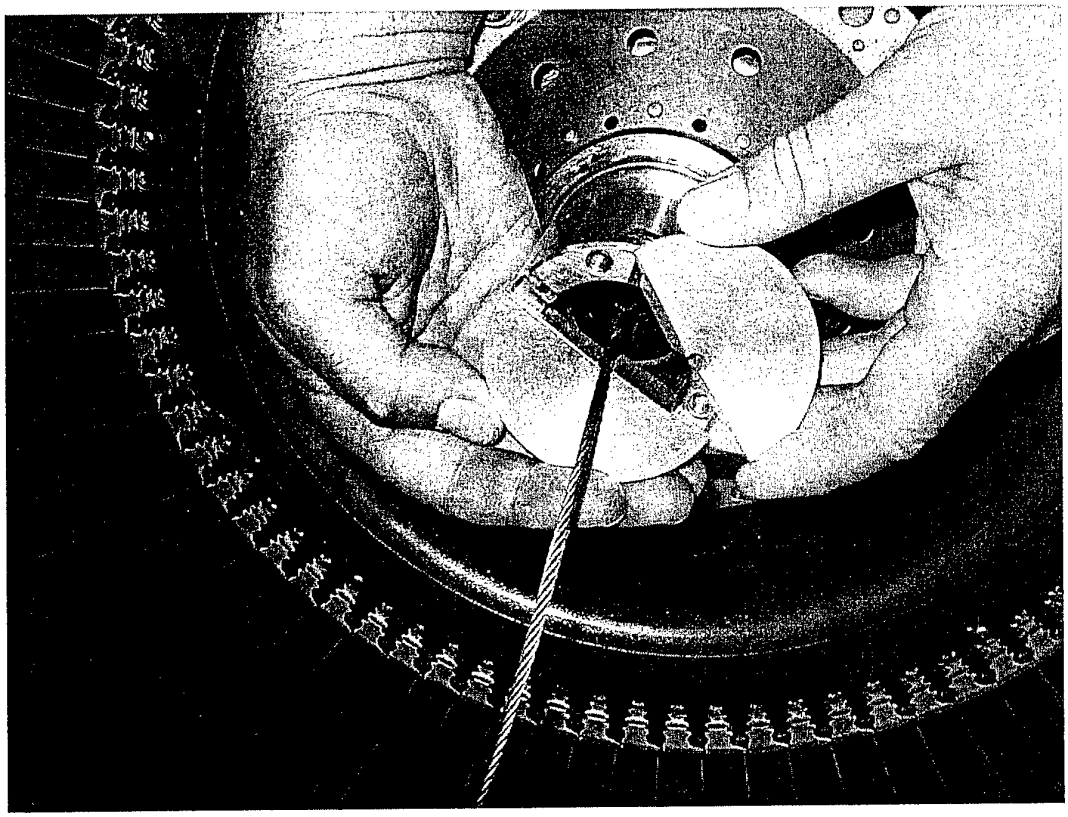

Figure 6. Cable centering spacer.

3.3 Rotor Excitation

The discrete frequency at which each bending mode vibration occurs is determined by the geometry, material, and mass distribution along the rotor. These natural

frequencies were excited by use of a sharp impulse, delivered with a wooden mallet, as shown in Figure 7. Because the energy of an impulse is spread over a wide frequency range, the vibration modes that occur at frequencies within this range will be excited.

For modal analysis using impulse excitation, in order to stimulate vibration that is of sufficiently high level to extract accurate vibration measurements over a wide frequency range, it may be necessary to strike the target hard with the mallet. As the rotors are high precision machined components, this method of excitation would not have been used if the rotors were flight-worthy and to be returned to serviceable stock.

3.4 Taking the measurements

The vibration of the excited rotor was measured using accelerometers, attached to the rotor with wax. Spectral analysis of the measured vibration shows several discrete vibration peaks. The orientation of the accelerometers was such that the measurement axis was perpendicular to the shaft axis, therefore the measured vibration can only be due to the natural bending motion of the vibrating shaft[2].

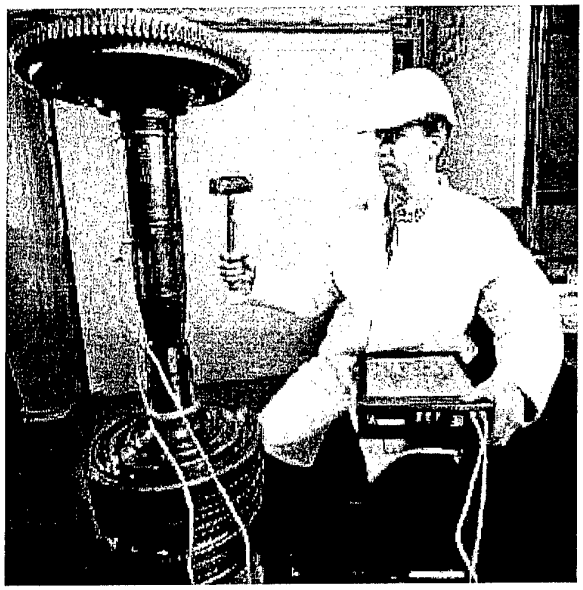

Figure 7. High speed rotor, with method of impulse excitation clearly visible.

The natural vibration bending modes of each discrete frequency were identified by using pairs of vibration readings from two accelerometers. The reference accelerometer was fixed at a reference location, while the roving accelerometer was moved to each designated measurement location for each reading. For each pair of vibration readings, the amplitude and phase of the vibration measured at the roving accelerometer was

[2] The pendulum motion of the shaft is far too low to be measured with the accelerometers used, and the bulk material compressive modes are likely to be much higher than the frequency range of interest.

accelerometer was calculated relative to the vibration of the reference accelerometer by use of transfer functions. That is:

$A^{i\phi}_{relative} = \frac{A^{i\phi}_{roving}}{A^{i\phi}_{reference}}$, where $A^{i\phi}$ is a complex number of amplitude A, and angle ϕ. The relative amplitude is calculated $A_{relative} = \frac{A_{roving}}{A_{reference}}$, and relative phase is calculated $\phi_{relative} = \phi_{roving} - \phi_{reference}$.

This was achieved using the transfer function capability of the CSI 2400 analyser. As the relative amplitude and phase is calculated for each designated measurement location on the shaft, a plot of the shape that the shaft is bending to can be generated.

4. Results

4.1 Low speed rotor

The first five bending modes of the low speed rotor were readily identifiable during measurement, and are illustrated here in Figures 8 - 12. For pure bending, it is expected that either 0° or 180° relative phase should be measured. This was indeed observed for the vast majority of readings, but there were 6 discrepancies in the 3rd, 4th, and 5th modes where the phase differed from 180° or 0° by more than 30°. These are most likely due to superposition of local modes at those locations.

Note that the measurement locations along the shaft were taken from the turbine end of the shaft.

Position along rotor (mm)	First Bending, @ 41.276 Hz	
	Amplitude (B/A)	Phase (deg)
2454	1.089	178
2157	0.3314	178
2042	0.0304	163
1907	0.303	1
1827	0.482	0
1717	0.833	0
1672	0.996	0
1531	1.035	0
1431	1.029	0
1331	1.0496	1
1231	1	0
1131	0.9435	1
1031	0.842	0
831	0.582	0
731	0.425	0
631	0.237	1
531	0.0564	9
431	0.14368	176
284	0.41	178
0	0.7382	179

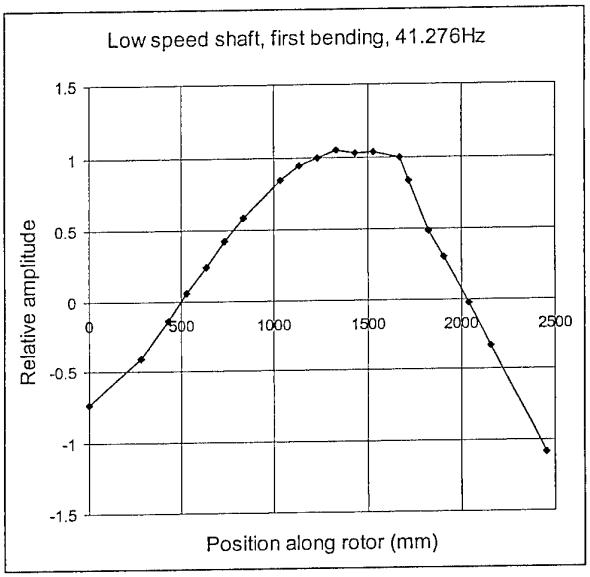

Figure 8. First bending mode of the N1 shaft, at 41.276 Hz.

Position along rotor (mm)	Second Bending, @ 125.72 Hz	
	Amplitude (B/A)	Phase (deg)
2454	0.5962	2
2157	0.0348	175
2042	0.28	-178
1907	0.544	-179
1827	0.682	-179
1717	0.946	-179
1672	0.964	-179
1531	0.185	-175
1431	0.23	-3
1331	0.6378	0
1231	1	0
1131	1.297	1
1031	1.482	0
831	1.518	1
731	1.354	1
631	1.0914	1
531	0.77045	1
431	0.4016	2
284	0.297	-179
0	1.149	-179

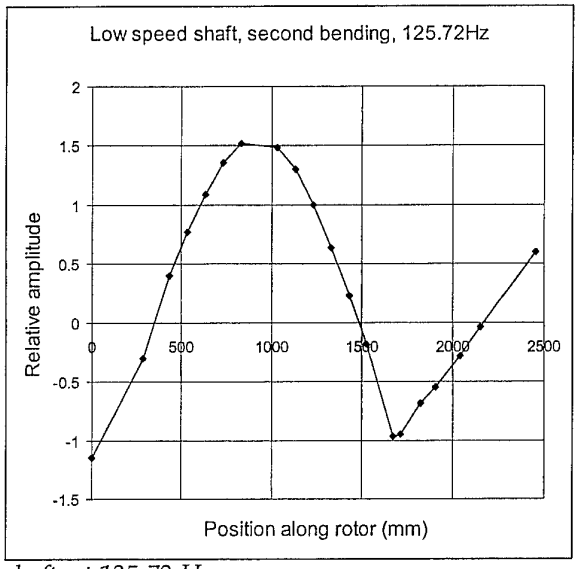

Figure 9. Second bending mode of the N1 shaft, at 125.72 Hz.

Position along rotor (mm)	Third Bending, @ 292.69 Hz	
	Amplitude (B/A)	Phase (deg)
2454	0.179	1
2157	0.0475	-176
2042	0.127	-178
1907	0.199	180
1827	0.213	-179
1717	0.293	-179
1672	0.203	175
1531	0.476	0
1431	0.7572	-1
1331	0.9492	0
1231	1	0
1131	0.914	2
1031	0.725	1
831	0.117	0
731	0.155	-179
631	0.35289	179
531	0.4738	-179
431	0.464	-178
284	0.0027	87
0	0.76737	0

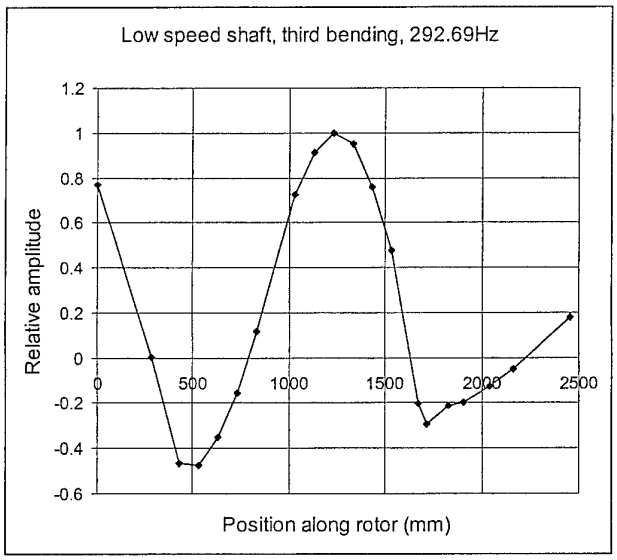

Figure 10. Third bending mode of the N1 shaft, at 292.69 Hz.

Position along rotor (mm)	Fourth Bending, @ 510.33 Hz	
	Amplitude (B/A)	Phase (deg)
2454	0.357	1
2157	0.238	-165
2042	0.287	-178
1907	0.354	-179
1827	0.286	179
1717	0.335	179
1672	0.0578	151
1531	1.4416	-1
1431	1.739	-1
1331	1.615	0
1231	1	0
1131	0.183	6
1031	0.714	178
831	1.685	179
731	1.544	-179
631	1.1208	179
531	0.5422	-179
431	0.00796	-30
284	0.1802	-3
0	0.2141	179

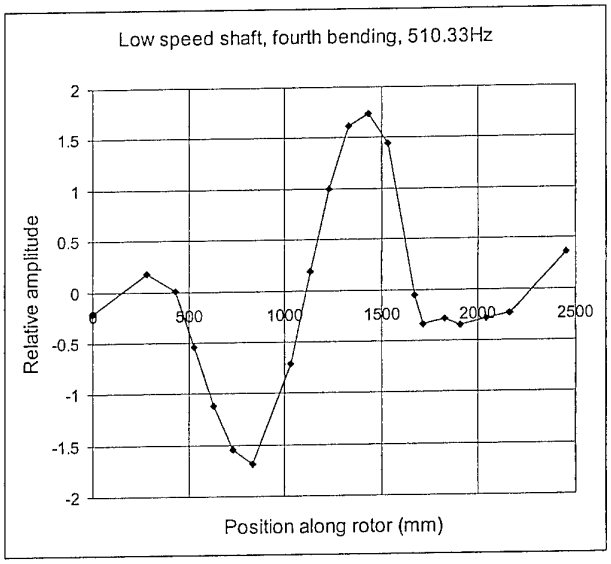

Figure 11. Fourth bending mode of the N1 shaft, at 510.33 Hz.

Position along rotor (mm)	Fifth Bending, @ 973.75 Hz	
	Amplitude (B/A)	Phase (deg)
2454	0.3325	4
2157	0.274	-175
2042	0.169	-176
1907	0.109	99.5
1827	0.323	3
1717	0.708	-2
1672	0.1115	-70
1531	2.069	-178
1431	1.648	-172
1331	0.461	-171
1231	1	0
1131	1.842	3
1031	1.834	2
831	0.536	179
731	1.527	-177
631	1.734	-176
531	1.453	-176
431	0.6776	-178
284	0.0907	113
0	0.1219	7

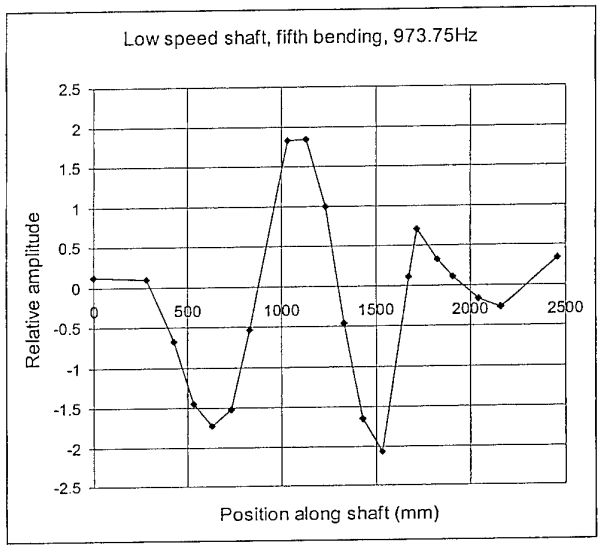

Figure 12. Fifth bending mode of the N1 shaft, at 973.75 Hz.

4.2 High speed rotor

The first two bending modes were readily identifiable during measurement on the high speed rotor, and are shown here in Figures 13 and 14.

Note that the measurement locations along the shaft were taken from the compressor end of the shaft.

Position along rotor (mm)	First Bending, @ 144.46 Hz	
	Amplitude (B/A)	Phase (deg)
Freq (Hz)	144.46	
35	0.7765	-180
131	0.25174	-179
216	0.20515	0
301	0.55736	0
388	0.91859	0
476	1.1915	0
571	1.3634	1
686	1.256	1
806	1	0
921	0.65467	0
1001	0.3649	0
1056	0.15123	-1
1173	0.34464	-179

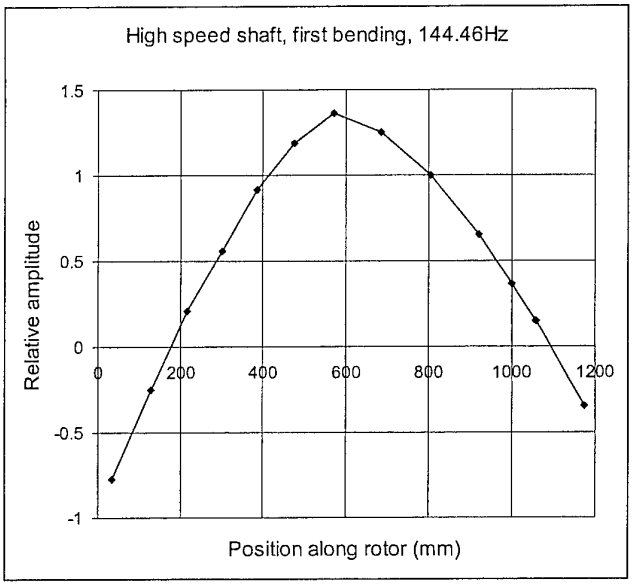

Figure 13. First bending mode of the N2 shaft, at 144.46 Hz

Position along rotor (mm)	Second Bending, @ 371.48 Hz	
	Amplitude (B/A)	Phase (deg)
Freq (Hz)	371.48	
35	0.339	2
131	0.01873	-7
216	0.25005	-172
301	0.44922	-179
388	0.5706	-179
476	0.31649	-178
571	0.077744	-6
686	0.62275	0
806	1	0
921	1.0816	1
1001	0.95496	1
1056	0.77092	1
1173	0.12539	-180

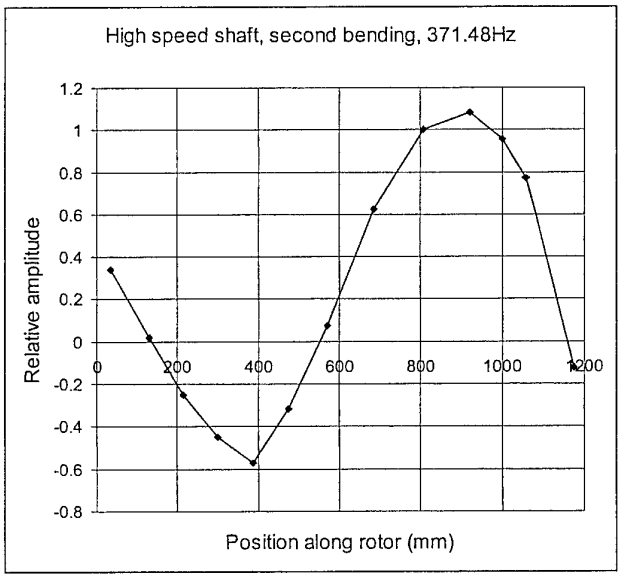

Figure 14. Second bending mode of the N2 shaft, at 371.48 Hz

5. Summary

Modal analysis was performed on the high and low speed TF30 P103 engine rotors in order to identify the shape and frequencies of the bending modes. The measurements were taken for the purpose of validating 3D finite element models of the rotors.

To facilitate assembly and handling of the complete shafts, they were assembled without any of the compressor or turbine blades installed. In addition, the low speed shaft assembly excluded the oil/air transfer tube, while the high speed shaft assembly excluded the turbine shaft lock, tie rod shield (rear compressor), and turbine air seal.

As these components are very light compared to the shaft weight, and they do not add to the structural stiffness of the shafts, the effect on the natural bending modes is judged to be minimal.

The modal measurements provide an unequivocal reference for the frequencies of the first five bending modes of the low speed shaft, and the first two bending modes of the high speed shaft. These measurements can be used to verify the accuracy of finite element models of the TF30 rotors.

6. Acknowledgement

The authors would like to thank Mr. David Dyett for his patience and skill in assembling the TF30 rotor assemblies, and FSGT Chris Buley and Mr Wayne Cooper of 501 WG RAAF Amberley for their patience in collecting the rotor components for our use.

DISTRIBUTION LIST

Measurement of the Natural Bending Modes of Rotors in the TF30 Engine

Mark Shilo and Andrew Becker

AUSTRALIA

DEFENCE ORGANISATION

Task Sponsor
FLTLT Adam Grey, SCI 4A

S&T Program
Chief Defence Scientist
FAS Science Policy
AS Science Corporate Management
Director General Science Policy Development
(shared copy)
Counsellor Defence Science, London (Doc Data Sheet)
Counsellor Defence Science, Washington (Doc Data Sheet)
Scientific Adviser to MRDC Thailand (Doc Data Sheet)
Scientific Adviser Joint
Navy Scientific Adviser (Doc Data Sheet and distribution list only)

Scientific Adviser - Army (Doc Data Sheet and distribution list only)

Air Force Scientific Adviser

Aeronautical and Maritime Research Laboratory
Director

Chief of Airframes and Engines Division
Research Leader: S. A. Fisher
Bryon Wicks
Jian Fu Hou
Albert Wong
Brian Rebbechi
Paul Marsden
David Blunt
Author(s): Mark Shilo
Andrew Becker

DSTO Library and Archives
Library Fishermans Bend (Doc Data Sheet)
Library Maribyrnong (Doc Data Sheet)
Library Salisbury (1 copy)
Australian Archives

US Defense Technical Information Center, 2 copies
UK Defence Research Information Centre, 2 copies
Canada Defence Scientific Information Service, 1 copy

NZ Defence Information Centre, 1 copy
National Library of Australia, 1 copy

Capability Systems Staff
Director General Maritime Development (Doc Data Sheet only)
Director General Aerospace Development

Knowledge Staff
Director General Command, Control, Communications and Computers (DGC4) (Doc Data Sheet only)

Army
Stuart Schnaars, ABCA Standardisation Officer, Tobruk Barracks, Puckapunyal, 3662 (4 copies)
SO (Science), Deployable Joint Force Headquarters (DJFHQ) (L), MILPO Gallipoli Barracks, Enoggera QLD 4052 (Doc Data Sheet only)

Air Force
Team Leader TST, 501WG, RAAF Amberley: Mr Greg Mason

Intelligence Program
DGSTA Defence Intelligence Organisation
Manager, Information Centre, Defence Intelligence Organisation

Corporate Support Program
Library Manager, DLS-Canberra

UNIVERSITIES AND COLLEGES
Australian Defence Force Academy
Library
Head of Aerospace and Mechanical Engineering
Hargrave Library, Monash University (Doc Data Sheet only)
Librarian, Flinders University

OTHER ORGANISATIONS
NASA (Canberra)
AusInfo

OUTSIDE AUSTRALIA

ABSTRACTING AND INFORMATION ORGANISATIONS
Library, Chemical Abstracts Reference Service
Engineering Societies Library, US
Materials Information, Cambridge Scientific Abstracts, US
Documents Librarian, The Center for Research Libraries, US

INFORMATION EXCHANGE AGREEMENT PARTNERS
Acquisitions Unit, Science Reference and Information Service, UK
Library - Exchange Desk, National Institute of Standards and Technology, US
National Aerospace Laboratory, Japan (

National Aerospace Laboratory, Netherlands

SPARES (5 copies)

Total number of copies: 51

DEFENCE SCIENCE AND TECHNOLOGY ORGANISATION
DOCUMENT CONTROL DATA

1. PRIVACY MARKING/CAVEAT (OF DOCUMENT)

2. TITLE

Measurement of the Natural Bending Modes of Rotors in the TF30 Engine

3. SECURITY CLASSIFICATION (FOR UNCLASSIFIED REPORTS THAT ARE LIMITED RELEASE USE (L) NEXT TO DOCUMENT CLASSIFICATION)

Document	(U)
Title	(U)
Abstract	(U)

4. AUTHOR(S)

Mark Shilo and Andrew Becker

5. CORPORATE AUTHOR

Aeronautical and Maritime Research Laboratory
506 Lorimer St
Fishermans Bend, 3207, Vic. Australia

6a. DSTO NUMBER	6b. AR NUMBER	6c. TYPE OF REPORT	7. DOCUMENT DATE
DSTO-TN-0393	AR-012-009	Technical Note	September, 2001

8. FILE NUMBER	9. TASK NUMBER	10. TASK SPONSOR	11. NO. OF PAGES	12. NO. OF REFERENCES
M1/9/939	00/147	DGTA SCI4A	12	1

13.: URL ON WORLDWIDE WEB

http://www.dsto.defence.gov.au/corporate/reports/DSTO-TN-0393.pdf

14. RELEASE AUTHORITY

Chief, Airframes and Engines Division

15. SECONDARY RELEASE STATEMENT OF THIS DOCUMENT

Approved for public release

OVERSEAS ENQUIRIES OUTSIDE STATED LIMITATIONS SHOULD BE REFERRED THROUGH DOCUMENT EXCHANGE, PO BOX 1500, SALISBURY, SA 5108

16. DELIBERATE ANNOUNCEMENT

No Limitations

17. CASUAL ANNOUNCEMENT Yes

18. DEFTEST DESCRIPTORS

Bending; Rotary wings; Rotors; Helicopters; Mechanical tests; TF-30 engines; Finite element method

19. ABSTRACT

The natural bending modes of the high and low speed shafts from the TF30 engine were measured i order to provide an unequivocal reference for validation of 3D Finite Element models of the shafts. Th shafts were assembled separately, and without blades or any engine casing structure.